

# Formation of hypermatter and hypernuclei within transport models in relativistic ion collisions.

A.S. Botvina<sup>1,2</sup>, J. Steinheimer<sup>1</sup>, E. Bratkovskaya<sup>1</sup>, M. Bleicher<sup>1</sup>, J. Pochodzalla<sup>3,4</sup>

<sup>1</sup>*Frankfurt Institute for Advanced Studies, J.W.Goethe University, D-60438 Frankfurt am Main, Germany*

<sup>2</sup>*Institute for Nuclear Research, Russian Academy of Sciences, 117312 Moscow, Russia*

<sup>3</sup>*Helmholtz-Institut Mainz, J.Gutenberg-Universität, 55099 Mainz, Germany*

<sup>4</sup>*Institut für Kernphysik and PRISMA Cluster of Excellence, J.Gutenberg-Universität Mainz, D-55099 Germany*

---

## Abstract

Within a combined approach we investigate the main features of the production of hyper-fragments in relativistic heavy-ion collisions. The formation of hyperons is modelled within the UrQMD and HSD transport codes. To describe the hyperon capture by nucleons and nuclear residues a coalescence of baryons (CB) model was developed. We demonstrate that the origin of hypernuclei of various masses can be explained by typical baryon interactions, and that it is similar to processes leading to the production of conventional nuclei. At high beam energies we predict a saturation of the yields of all hyper-fragments, therefore, this kind of reactions can be studied with high yields even at the accelerators of moderate relativistic energies.

**Keywords:** Hypernuclei, relativistic heavy-ion reactions, nuclear fragments production

---

## 1. Introduction

The investigation of hypernuclei is a rapidly progressing field of nuclear physics, since these nuclei provide complementary methods to improve traditional nuclear studies and open new horizons for studying nuclear physics aspects related to particle physics and nuclear astrophysics (see, e.g., [1, 2, 3, 4, 5, 6, 7, 8] and references therein). Indeed, baryons with strangeness embedded in a nuclear environment are the only available tool to approach the many-body aspects of the three-flavor strong interaction. Hyperon-nucleon and hyperon-hyperon interactions are also an essential ingredient for the nuclear Equation of State (EOS) at high density and low temperature. Another novel aspect of contemporary hypernuclear studies is the exploration of the limits of stability in isospin and strangeness space.

Presently, hypernuclear physics is still focused on spectroscopic information and is dominated by a quite limited set of reactions. These are reactions induced by high-energy hadrons and leptons leading to the production of only few particles, including kaons which are often used to tag the production of hypernuclei in their ground and low excited states. In such reactions hyper-systems with baryon density around the nuclear saturation density,  $\rho_0 \approx 0.15 \text{ fm}^{-3}$  are formed. Therefore, most previous theoretical studies concentrated on the calculation of the structure of nearly cold hypernuclei. However, many experimental collaborations (e.g., PANDA [9], FOPI/CBM, and Super-

FRS/NUSTAR at FAIR [10, 11]; STAR at RHIC [12]; ALICE at LHC [13]; BM@N and MPD at NICA [14]) have started or plan to investigate hypernuclei and their properties in hadron and heavy ion induced reactions. This represents an essential extension of nuclear/hypernuclear studies: The isospin space, particle unstable states, multiple strange nuclei, the production of hypermatter, and precision lifetime measurements are unique topics of these fragmentation reactions.

It is relevant in this respect to note that the very first experimental observation of a hypernucleus was obtained in the 1950-s in nuclear multifragmentation reactions induced by cosmic rays [15]. In recent years a remarkable progress was made in the investigation of the fragmentation and multifragmentation reactions associated with relativistic heavy-ion collisions (see, e.g., [16, 17, 18, 19, 20] and references therein). This gives us an opportunity to apply well known theoretical methods, which were adopted for the description of the conventional reactions, also for the formation of hypernuclei [21, 22]. The task of this work is to develop new realistic models of hypernuclear production which are able to provide detailed predictions in order to optimise the experimental conditions when searching for both  $\Lambda$ -hypernuclei and normal exotic nuclei.

The formation processes of hypernuclei are quite different in central and peripheral ion collisions. There are indications that in high energetic central collisions the coalescence mechanism, which assemble light hyper-fragments from the produced hyperons and nucleons (including anti-

baryons) is dominating [12, 13, 23, 24]. Because of the very high temperature of the fireball ( $T \approx 160$  MeV) only lightest clusters, with mass numbers  $A \lesssim 4$ , can be produced in this way with a reasonable yield [25]. On the other hand, it was noticed sometime ago that the capture of hyperons in spectator regions after peripheral nuclear collisions is a promising way to produce hypernuclei [26, 27, 28, 29]. Nuclear matter created in peripheral collisions shows distinctly different properties compared to nuclear matter at mid-rapidity. It is well established that moderately excited spectator residues ( $T \lesssim 5-6$  MeV) are produced in such reactions [16, 17, 18, 30]. A hyperon bound in these residues should not change the picture since the hyperon-nucleon forces are of the same order as the nucleon-nucleon ones. General features of the decay of such hyper-residues into hyper-fragments could be investigated with statistical models (e.g., generalized Statistical Multifragmentation Model SMM [7, 21]), which successfully describe the production of normal fragments [16, 17, 18, 19]. The models predict the formation of exotic hypernuclei and hypernuclei beyond the drip-lines, which are difficult to create in other reactions [7]. There is an alternative treatment of the process that considers first statistical SMM decay of excited residues, and, afterwards, a coalescence model for final production of hyper-fragments [28]. Both theoretical mechanisms are under discussion and waiting for a test by experiments. Spectator heavy fissioning hypernuclei were identified with a relatively high probability in reactions induced by protons with energy around the threshold [31], and in annihilation of antiprotons [32]. Very encouraging results on hypernuclei come from experiments with light projectiles: In addition to well-known hypernuclei [33], evidences for unexpected exotic hypernuclear states, like a  $\Lambda$  hyperon bound to two neutrons, were reported [34], which were never observed in other reactions. As was discussed, the production of such new exotic states could be naturally explained within the break-up of excited hypernuclear systems [34, 35].

In previous publications we have considered the formation of hypernuclei within the Dubna cascade model (DCM) [36, 37] and the Ultra-relativistic Quantum Molecular Dynamics model (UrQMD) [38]. These calculations include the capture of the produced hyperons in the potential of the spectator residues [29, 39], and the coalescence into lightest clusters together with their thermal production in central collisions [25]. Involving new transport models is very important since we obtain knowledge about uncertainties in such calculations. In this work, besides UrQMD, we employ the hadron-string dynamics (HSD) model [40], which were used successfully for description of strangeness production [41, 42]. We develop a generalization of the coalescence model [43], the coalescence of baryons (CB), which is applied after UrQMD and HSD stage. In this way it is possible to form fragments of all sizes, from the lightest nuclei to the heavy residues, including hypernuclei within the same mechanism. The advantage of this procedure is the possibility to predict the

correlations of yields of hypernuclei, including their sizes, with the rapidity on the event-by-event basis, that is very essential for the planning of future experiments.

## 2. Transport calculations of conventional and strange baryons

A detailed picture of peripheral relativistic heavy-ion collisions has been established in many experimental and theoretical studies. Nucleons from the overlapping parts of the projectile and target (participant zone) interact intensively between each other and with other hadrons produced in primary and secondary collisions. Nucleons from the non-overlapping parts interact rarely, and they form the residual nuclear systems, which we call spectators. We apply two dynamical models to describe the processes leading to the production of strange particles in nucleus-nucleus collisions before their accumulation in nuclear matter. Using different models allows us to estimate the theoretical uncertainties associated with the different treatment of the dynamical stage.

The first model is the Ultra-relativistic Quantum Molecular Dynamics model (UrQMD) [38, 44]. The model is based on an effective microscopic solution of the relativistic Boltzmann equation. Products of binary interactions of particles include 39 different hadronic species (and their anti-particles) which scatter according to their geometrical cross section. The allowed processes include elastic scattering and  $2 \rightarrow n$  processes via resonance creation (and decays) as well as string excitations for large center-of-mass energies ( $\sqrt{s} \gtrsim 3$  GeV). The current version 3.4 of UrQMD also includes important strangeness exchange reactions, e.g.,  $\bar{K} + N \leftrightarrow \pi + Y$  (where  $Y$  is a strange baryon) [45].

Another model is the off-shell Hadron-String-Dynamics (HSD) transport model [40, 46]. It is based on the solution of the generalized transport equation [47] including covariant self energies for the baryons. We recall that in the HSD approach nucleons,  $\Delta$ 's,  $N^*(1440)$ ,  $N^*(1535)$ ,  $\Lambda$ ,  $\Sigma$  and  $\Sigma^*$  hyperons,  $\Xi$ 's,  $\Xi^*$ 's and  $\Omega$ 's as well as their antiparticles are included on the baryonic side, whereas the  $0^-$  and  $1^-$  octet states are incorporated in the mesonic sector. Inelastic baryon-baryon (and meson-baryon) collisions with energies above  $\sqrt{s_{th}} \simeq 2.6$  GeV (and  $\sqrt{s_{th}} \simeq 2.3$  GeV, respectively) are described by the FRITIOF string model [48], whereas low energy hadron-hadron collisions are modelled using experimental cross sections.

In the both HSD and UrQMD models the initial state of colliding nuclei is generated similarly: The nucleon's coordinates are initialized according to a Woods-Saxon profile in coordinate space and their momenta are assigned randomly according to the Fermi distribution.

## 3. Coalescence of baryons

A composite particle can be formed from two or more nucleons if they are close to each other in phase space. This

simple prescription is known as coalescence model and it is based on the properties of the nucleon–nucleon interaction. One can use the coalescence in both momentum (velocity) space and the coordinate space. The coalescence in the momentum space model has proven successful in reproducing experimental data on the production of light clusters (see e.g. [25, 36]).

Recently, we developed an alternative formulation of the coalescence model, the coalescence of baryons (CB), which is suitable for computer event by event simulations [43]. Baryons (nucleons and hyperons) can produce a cluster with mass number  $A$  if their velocities relative to the center-of-mass velocity of the cluster is less than  $v_c$ . Accordingly we require  $|\vec{v}_i - \vec{v}_{cm}| < v_c$  for all  $i = 1, \dots, A$ , where  $\vec{v}_{cm} = \frac{1}{E_A} \sum_{i=1}^A \vec{p}_i$  ( $\vec{p}_i$  are momenta and  $E_A$  is the sum energy of the baryons in the cluster). This is performed by sequential comparison of the velocities of all baryons.

If we consider only the production of lightest clusters ( $A \lesssim 4$ ) the coalescence velocity parameter  $v_c \approx 0.1c$  gives a good description of the data, as was shown in previous analyses [25, 36]. However, the coalescence mechanism may also be applied to construct heavy nuclei [43]. In this case the parameter  $v_c$  should be larger, in order to incorporate higher velocities of the hyperons which can be captured in the deeper potentials of big nuclei. This potential well saturates at around  $\sim 30$ – $40$  MeV. It was demonstrated in Ref. [29] (fig. 10) that according to this potential criterion the momentum distribution of the captured  $\Lambda$  hyperons can be approximated by a step-like function, and that hyperons with relative momenta less than  $200$ – $250$  MeV/c can be bound. Therefore, relative velocities up to  $0.25c$  should be taken into account as coalescence parameter, which is naturally close to the Fermi velocity.

We would like to note a problem which is sometimes disregarded in coalescence simulations. Some nucleons may have velocities such that they can belong to different (or even more than two) coalescent clusters according to the coalescence criterion. In these cases the final yield will depend on the sequence of nucleons within the algorithm. To avoid this uncertainty we developed an iterative coalescence procedure.  $M$  steps are calculated in the coalescence routine with the radius  $v_{cj}$  which is increased at each step  $j$ :  $v_{cj} = (j/M) \cdot v_c$  (with  $j = 1, \dots, M$ ). Clusters produced at earlier steps participate as a whole in the following steps. In this case the final clusters not only meet the coalescence criterion but also their nucleons have the minimum distance in the velocity space. This procedure gives a mathematically correct result in the limit  $M \rightarrow \infty$ , however, we found that in practical calculations it is sufficient to confine the steps to  $M=5$ .

For more reliable identification of the clusters, we apply in addition a coordinate proximity criterion. A single baryon and a cluster with mass number  $A$  is confirmed to compose the new cluster if the relative distances of all baryons from the cluster's center of mass  $r_c$  is less

than  $r_0 \cdot (A+1)^{1/3}$ . Here is  $r_0=2$  fm, which can be justified by multifragmentation studies (see, e.g., [16]): It was established that an excited nuclear system (with mass  $A$ ) before its disintegration may reach a big freeze-out volume  $\approx 4/3\pi r_0^3 A$ . In this volume the system can be considered in thermal equilibrium and live for a short time ( $\sim 100$  fm/c). We assume that the coalescence should be a rather fast process which happens when particles leave the interaction zone and the rate of the secondary interactions decreased considerably. From the UrQMD model calculation for  $20$  A GeV we evaluate this time as  $\lesssim 50$  fm/c for big targets and projectiles [29]. That is usually smaller than the decay time of nuclear systems in both multifragmentation and evaporation/fission processes: It is therefore naturally that such a coalescence prescription may introduce an excitation energy in the clusters, which can decay afterwards. As our analysis shows, the criterion in the coordinate space correlates with the velocity criterion. Namely, when the projectile and target are well separated at later times of the reaction, the proximity in the velocity space means the proximity in the coordinate space too. This correlation appears naturally within the potential capture criterion [29].

Another important development of our coalescence procedure is that we assign the primary nucleons of initial nuclei to the residual nuclei if they did not interact with any particle during the collision. In some approaches these residues are formed by default [36, 29]. However, in the transport models used here (UrQMD, HSD) these nucleons preserve initialized momenta. The stability of the initial nuclei is not pursued in this case, since low-energy interactions inside nucleus are not precisely determined. We think it is a very good approximation to combine such nucleons into a residual cluster, especially for peripheral collisions, because of their initial proximity in momentum and coordinate space. We have checked that it is not effective to resolve the residues' problem by simply increasing the coalescence parameters within our procedure, since we would enforce artificially the formation of the lightest clusters too. In addition we verify the assignment of these nucleons to the residues by controlling their rapidities  $y$ : Most nucleons deviate by less than  $\pm 0.267$  from the rapidities of the target and projectile. (This range  $\Delta y = 0.267$  is associated with the Fermi momenta of nucleons in the initial nucleus [29].) As we know from the production of normal fragments [17, 18, 19], the realistic description of residues is important: According to the general picture of these reactions [21], many hyperons can be captured by a sufficiently large piece of excited spectator matter, leading to the formation of hot hypermatter, which in the following decay via evaporation, Fermi-break-up, fission, or multifragmentation.

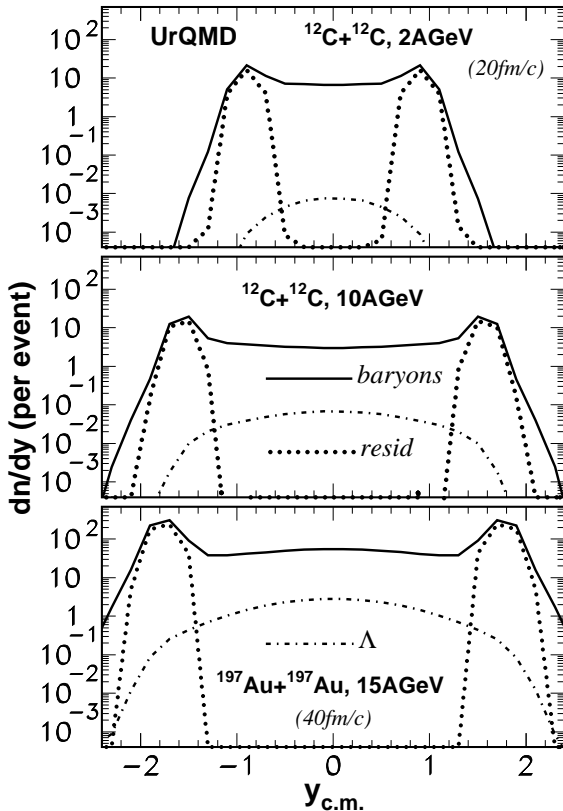


Figure 1: UrQMD calculations for rapidity distributions of all baryons (solid lines), non-interacting spectator nucleons (dotted lines) and  $\Lambda$  hyperons (dot-dashed lines), produced in collisions of carbon and gold beams with all impact parameters, normalized per inelastic event. The projectile energies and the times after the maximum overlap between the target and projectile are shown in the panels.

#### 4. Rapidity and mass distributions of fragments and hyper-fragments

For our analysis we have selected both small and heavy colliding nuclei, however, symmetric systems. For carbon projectile and targets we have performed calculations for different energies which are relevant for GSI/FAIR facility [49, 50]. The reason is that the light hypernuclei can be quite easily identified in future experiments, and that such experiments are already planned [11]. The reactions with gold nuclei are added to generalize our conclusions for the production of heavy fragments at high beam energy. Such energies are easily reached with available accelerators (in particular, RHIC) and our predictions can help to prepare measurements of both light and heavy hypernuclei at all possible rapidities. We generated from  $10^4$  to  $10^6$  inelastic events for each energy while integrating over all impact parameters ('minimal' bias calculations).

For collisions of light (carbon) nuclei we stop our transport calculations at the time moment of 20 fm/c after the

maximum overlap between the target and projectile has been reached. We have checked that at later time cuts the number of produced particles and their momenta change very little, since they are far separated from each other. The result of the coalescence process remains nearly the same if we increase this time scale. For the gold nuclei the corresponding time was taken as 40 fm/c, since they are larger.

In Fig. 1 we show the UrQMD results of the total rapidity distributions of all baryons and  $\Lambda$  hyperons produced in the collisions of a carbon projectile and target with laboratory beam energies of 2 and 10 GeV per nucleon, and for a gold on gold system at 15 GeV per nucleon. We have specially separated the remaining spectator nucleons which participate mostly in producing fragments and hyper-fragments in the target and projectile region. The rapidity distributions obtained with HSD model have practically the same form. One can see wide baryon and hyperon distributions which cover the whole rapidity range of the reaction. The peaks at projectile and target rapidities do mainly consist of the spectator nucleons which did not interact and which form the residues. All these particles are both the output of the transport models and the input for the coalescence approach leading to formation of nuclear and hyper-nuclear matter. Large excited pieces of hyper-matter can be produced by the capture of  $\Lambda$  hyperons within the nuclear residues, as demonstrated also in Ref. [29]. Similar to nuclear reactions without the involvement of strange particles, we expect that these hyper-residues will be excited and decay afterwards [21] producing final nuclei and hypernuclei. However, the formation of light hyper-clusters can take place at all rapidities. This is an advantage of the coalescence procedure as it can account for all these phenomena on the same footing, and, therefore, systematic comparisons can be performed.

The total mass yields of the normal fragments and hyper-fragments (with one bound  $\Lambda$ ) are shown in Fig. 2. The coalescence of baryons (the CB model) was applied after the UrQMD, for the reactions demonstrated in Fig. 1. The yields are normalized per one inelastic event. However, one should take into account that only events with production of hyperons have been analysed in this case. For this reason there is no characteristic increase of the yield of normal fragments with masses around the projectile/target mass, which are caused by very peripheral collisions. The explanation of this behaviour was already suggested in Ref. [29]: The production of hyperons needs usually many particle collisions leading to a considerable emission of fast nucleons from the residues. The HSD+CB calculations show similar distributions.

One can see that the production of fragments of all sizes is possible. As expected the yield of conventional fragments is by few orders of magnitude higher than the yield of hyper-fragments. Nevertheless, the production of hyper-fragments is sufficient to be experimentally measured (see also [39]). It is a natural result of the coalescence that the yield of the lightest hyper-fragments is dominating.

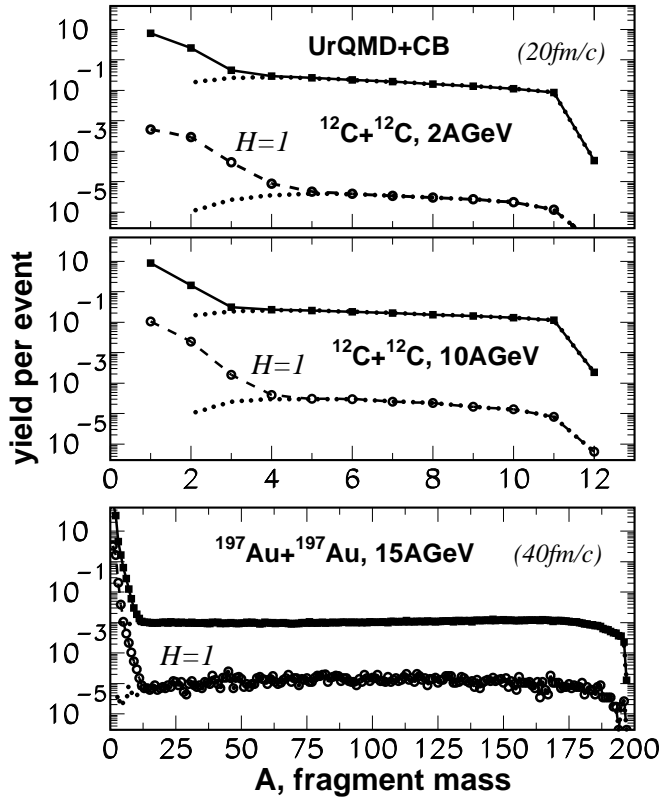


Figure 2: Yields (per one inelastic event) of normal fragments (solid lines with squares) and hyper-fragments with one captured  $\Lambda$  (notation  $H=1$ , dashed lines with circles) versus their mass number ( $A$ ) in reactions induced by carbon and gold collisions. The dotted lines present the corresponding fragments originated from the spectator residues. The calculations are performed within the hybrid UrQMD plus CB model, with the coalescence parameter  $v_c = 0.22c$ , and integration over all impact parameters. The projectile lab energies and the transition times from UrQMD to CB are shown in panels.

However, the capture of hyperons by residues saturates the yield for large masses and leads to abundant production of heavy hyper-fragments. Within this approach one can see clearly that nearly all normal fragments and hyper-fragments with  $A > 3-4$  in the carbon collisions, and with  $A > 10$  in the gold collisions originate from the capture of  $\Lambda$  hyperons by spectator residues (dotted lines). As was mentioned we believe that these hyper-fragments represent excited pieces of hyper-matter whose evolution can be calculated with statistical models [21, 7]. The excitation energy of such primary fragments can also be evaluated from the analysis of experimental data [16, 17, 18, 19].

For this calculation we have used the coalescence parameter  $v_c = 0.22c$  in order to take into account the higher velocities possible in big clusters formed by the residues. It is also consistent with the values obtained in our previous

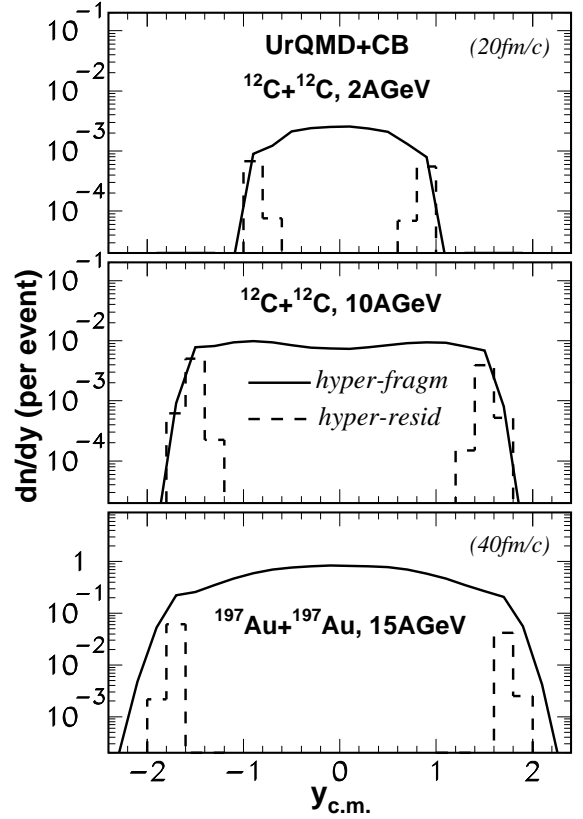


Figure 3: Rapidity distributions (in the center of mass system,  $y_{c.m.}$ ) of produced hyper-fragments (solid lines) and hyper-residues (dashed lines) calculated within the UrQMD plus CB model. The reactions, parameters and other notations are as in Fig. 2.

analysis in Ref. [29]. Decreasing  $v_c$  leads to a smaller yield of hyper-fragments, without changing the form of their distribution. In this case the yield of light normal fragments is reduced while residues are hardly affected.

To complement the analysis of the fragment masses we provide information about the velocities of all produced hyper-fragments. Here and in the following figures we consider the hyper-fragments and hyper-residues with mass numbers  $A > 2$ . Their total rapidity distributions are demonstrated in Figs. 3 and 4, for UrQMD+CB and HSD+CB calculations respectively. The hyper-fragments can be produced at any rapidity available for hyperons in the reaction (solid lines). However, as seen from the figures the big fragments, which can come only from the residues, are concentrated around the target and projectile rapidity (dashed lines). The small fragments formed after the coalescence of fast baryons can populate the midrapidity region also. As can be seen from a comparison of Fig. 3 and Fig. 4 the shape of the obtained distributions do not change with the employed transport models, UrQMD

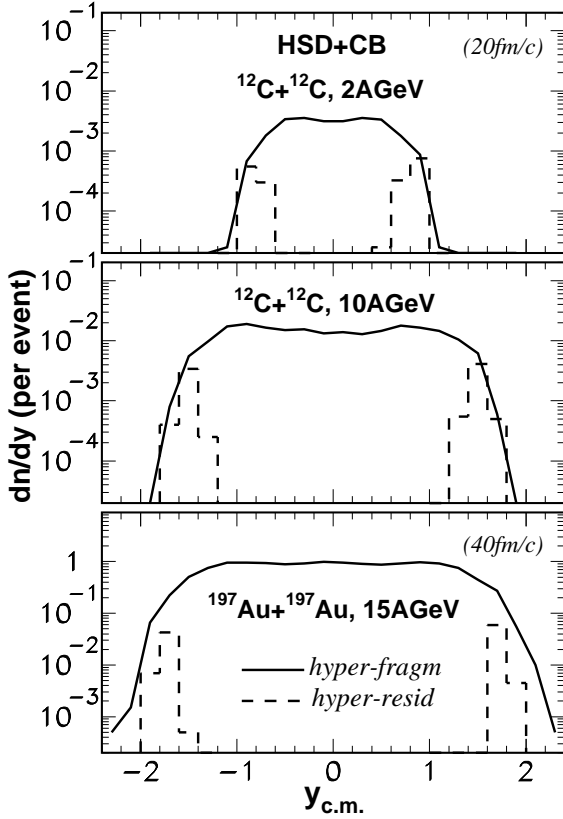


Figure 4: The same as in Fig. 3 but for calculations within the HSD plus CB model.

and HSD. However, the yields of light hyper-fragments are slightly larger in the HSD case. It is instructive that in the carbon collisions the hyper-residues are responsible for producing nearly all hyper-fragments in their kinematic regions. In the gold case, many new particles are produced in this region, therefore, besides big hyper-residues additional light hypernuclei can be formed too.

The light hypernuclei  ${}^3_{\Lambda}\text{H}$  and  ${}^4_{\Lambda}\text{H}$  are specially interesting: They can be easily identified by their decay into  $\pi^-$  and  ${}^3\text{He}$ , and into  $\pi^-$  and  ${}^4\text{He}$ , respectively. These correlations have been observed already in many heavy-ion experiments at high energies [12, 13, 23, 33, 34]. Such hypernuclei can serve as indicators for the production of hyper-matter.

In Figs. 5 and 6 we show the rapidity distributions of these light hypernuclei produced in the same reactions. The simulations are performed within the UrQMD and CB models. As before, the coalescence parameter  $v_c = 0.22c$  has been used for the calculations shown in Fig. 5. For comparison, the results obtained with a smaller parameter  $v_c = 0.1c$  are presented in Fig. 6. The latter may be more adequate for these small nuclei, since previously the yields of normal small clusters have been well described

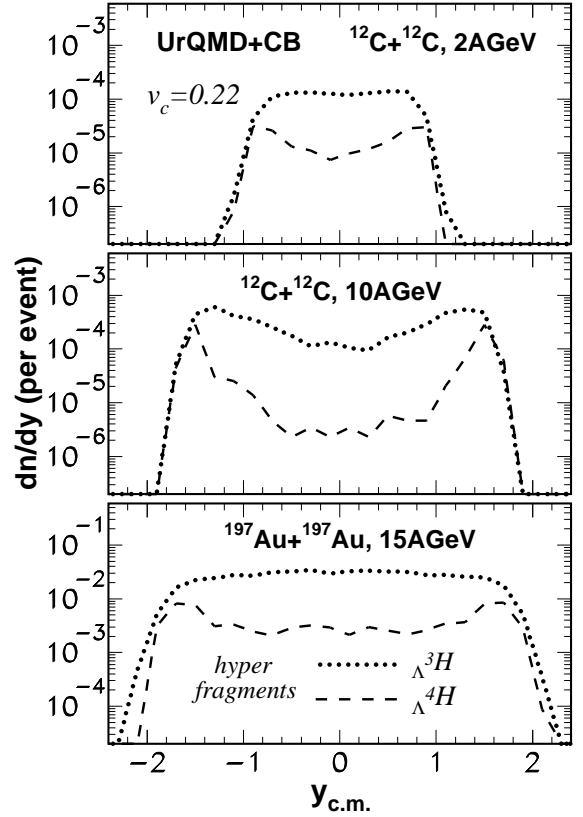


Figure 5: Rapidity distributions of produced  ${}^3_{\Lambda}\text{H}$  (dotted lines) and  ${}^4_{\Lambda}\text{H}$  (dashed lines) hyper-fragments in reactions as in Fig. 3. The UrQMD and CB calculations are with the coalescent parameter  $v_c = 0.22c$

with a such low coalescence parameter [25, 36]. In this case the fragments can be treated already as nuclei in final state without secondary de-excitation, since the later one is mainly relevant for big residues.

One can see an interesting behaviour: The  ${}^3_{\Lambda}\text{H}$  nuclei are essentially formed over all rapidities. It is obvious, that the production of the clusters is smaller at low coalescent parameters (compare Figs. 5 and 6). At low  $v_c$ , however, the fragments are more grouped at the target and projectile rapidities. This concentration is more evident for larger nuclei –  ${}^4_{\Lambda}\text{H}$ . This is the consequence of the applied coalescent mechanism: If the velocity space is reduced the large clusters are more efficient in the capture of hyperons because of the larger coordinate space.

With increasing energy the fraction of nuclei around residues increases, since more particles are produced in this region as a result of secondary interactions. Whereas particles originating from midrapidity have higher energy and they are more separated in the phase space. Therefore, despite of the general increase the number of such particles, the total number of clusters may not increase.

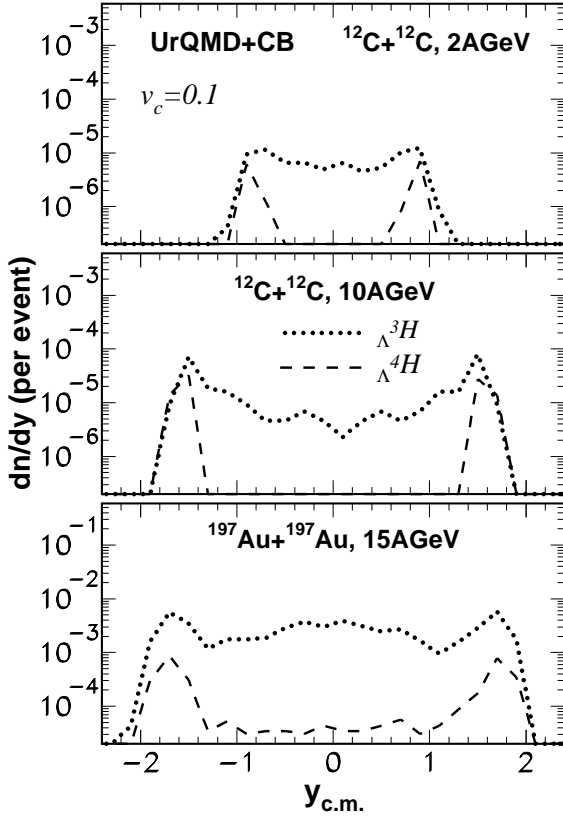


Figure 6: The same as in Fig. 5 but with the coalescent parameter  $v_c = 0.1c$

The dependence of the results on the coalescence parameter was specially investigated in these reactions, since it is related to the main uncertainty of the predictions. Figs. 7 and 8 show the total yields of hyper-fragments and hyper-residues in collisions of carbon on carbon, and gold on gold, respectively. As usual, the yields are normalized per inelastic event and integrated over all impact parameters. One can see that the UrQMD as well as the HSD model gives similar results. As expected all yields increase with  $v_c$ . However, at small  $v_c$  the capture of hyperons take place on residual nuclei predominantly. The big residues cover a large coordinate space region that becomes important for this mechanism in the case of reducing the momentum space. It is also essential that the secondary interactions which contribute considerably to the formation of hyperons with relatively low momenta happen mostly in the residue region. On the other hand, primary interactions leading to the production of high-energy hyperons take place in the central (midrapidity) region. In this case particles are far from each other in momentum space, therefore, in order to construct a cluster a larger  $v_c$  is required.

In the gold collisions the difference between the calcu-

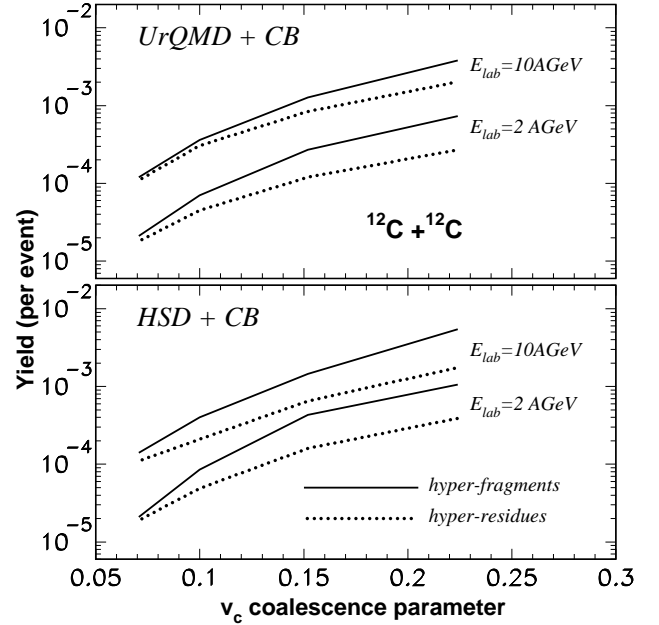


Figure 7: Yields of all produced hyper-fragments (solid lines) and hyper-residues (dotted lines) versus the coalescent parameter  $v_c$ , as calculated within the UrQMD and CB model (top panel) and HSD and CB model (bottom panel). The reaction is the carbon on carbon collisions (integrated over all impact parameters) with the projectile lab energies of 2 and 10 GeV per nucleon, see notations by the lines.

lations with UrQMD and HSD for light hyper-fragments is more prominent, by about a factor 2 (see Fig. 8). Within the models this is related to the treatment of the secondary interactions and HSD leads to an enlarged production of these hyper-fragments. However, the values predicted by both models look quite reasonable, and they can be checked by analysing experimental data. In turn, the possible variation of the predictions is important for planning future measurements.

Since increasing the beam energy results in a larger number of produced hyperons, the yields of hyper-fragments may increase too. This is clearly seen in Fig. 7. More details are shown in Fig. 9 for carbon collisions for a wide range of beam energies. There is a saturation of the yields of hyper-fragments, both light and heavy ones, at energies higher than 5–10 GeV per nucleon. This effect is found for both models and for all coalescent parameters. Depending on  $v_c$  this saturation happens at a different level. By comparing these results with the previous ones which were obtained with the DCM and the capture of hyperons by the nuclear potential (see Fig. 2 in Ref. [39]) we note that they will be similar if we take the values of  $v_c$  in-between the ones shown now in Fig. 9 (i.e., in-between 0.1 and 0.22). The uncertainty obtained with this parameter should be clarified by a comparison with experimental data and with more sophisticated theory calculations. Be-

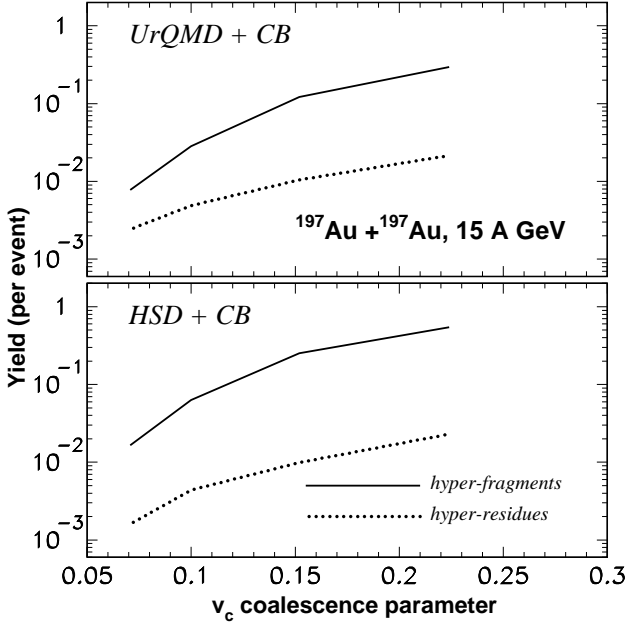


Figure 8: The same as in Fig. 7 but in the reaction of the gold on gold collision at 15 GeV per nucleon.

cause of the saturation of the yield at high energies the experimental hypernuclear studies can be pursued at the accelerators of moderate relativistic energies, above the threshold ( $\gtrsim 1.6$  A GeV).

Generally, this combination of the transport and coalescence models can be used for analysis of yields of non-strange fragments too. This can give an additional insight into the reaction mechanism. Besides light fragments which were already tested [25, 36], the intermediate and large fragments are also of considerable interest, e.g., see the ALADIN data [17, 19]. As mentioned, a detailed comparison may require a connection with the secondary de-excitation processes.

## 5. Conclusion

We conclude that relativistic heavy-ion reactions are a very promising source of hyper-matter and hyper-fragments. A large amount of hypernuclei of all masses can be produced. Their properties can also be investigated taking into account the advantages of relativistic velocities, e.g., for the life-time and correlation measurements.

The well established UrQMD and HSD transport models have been used in order to describe the strangeness and hyperon formation. They give a quite reliable picture of the reactions and they also consistent with other dynamical approaches (e.g., DCM) used by us previously. The interaction of hyperons with nucleons leads to their capture and to the formation of hyper-matter. We describe this process within a generalized coalescence model. The coalescence of baryons is consistent with the hyperon capture

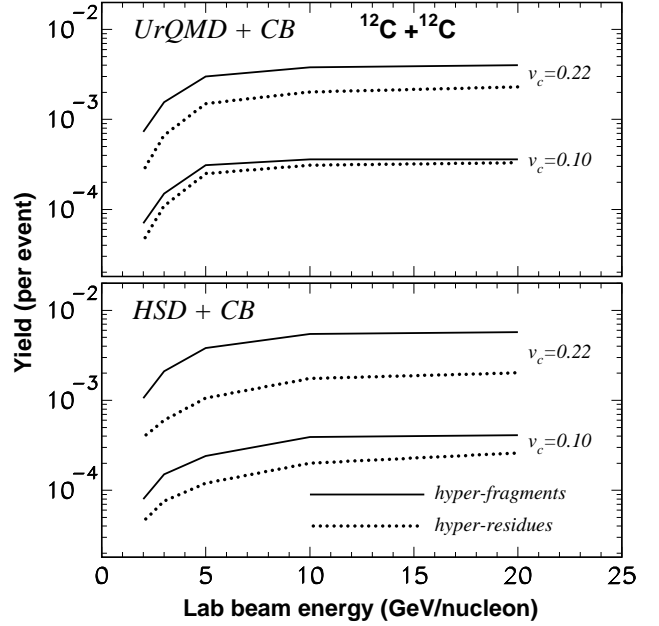


Figure 9: Yields of all produced hyper-fragments (solid lines) and hyper-residues (dotted lines) versus the beam energy in the carbon on carbon collisions for all impact parameters, as calculated within the UrQMD and CB model (top panel) and HSD and CB model (bottom panel). The coalescent parameters  $v_c$  are given in the panels.

in a potential well of large nuclear residues, and the coalescence parameters are expected to be of the same order as for normal fragments. This procedure gives a possibility to consider the formation of light hypernuclei on the same footing. We demonstrate that big hyper-fragments are mostly produced from the spectator residues, while the light ones can be formed at all rapidities. We expect, however, that some large species of hypermatter will be excited, and decay afterwards with production final hypernuclei and normal nuclei, as in usual fragmentation and multifragmentation reactions. Such a mechanism should allow the investigation of possible phase transitions in hypermatter with statistical models describing the secondary disintegration.

By summing up the results obtained with various models we note that the production of hyper-fragments in relativistic heavy-ion collisions is universal and well established theoretically. It is very instructive to investigate the whole reaction mechanism by measuring simultaneously big hypernuclei originating from the residues and light hypernuclei which can be formed in the hot midrapidity region. The saturation of all yields takes place at the beam energies higher than 5–10 GeV per nucleon. This opens the possibility to study hypernuclei at GSI/FAIR (Darmstadt), Nuclotron/NICA (Dubna), RHIC (Brookhaven), HIAF (Lanzhou) and other heavy-ion accelerators of moderate relativistic energies. In the following we plan to



analyze theoretically the formation of multi-hyperon nuclei, which can be abundantly produced in these reactions. Another promising opportunity would be to study unstable (resonance) states of hypernuclei via particle correlations. In addition, exotic hypernuclei may be formed and investigated in the secondary evaporation, fission, and multifragmentation-like processes. Comparing these theoretical predictions with future experiments may provide new information on the  $YN$  and  $YY$  interaction at low energies, as well as about properties of hyper-matter.

## 6. Acknowledgments

This work was supported by the the GSI Helmholtzzentrum für Schwerionenforschung and Hessian initiative for excellence (LOEWE) through the Helmholtz International Center for FAIR (HIC for FAIR). We also acknowledge the support by the Research Infrastructure Integrating Activity Study of Strongly Interacting Matter HadronPhysics3 under the 7th Framework Programme of EU (SPHERE network). The computational resources were provided by the LOEWE Frankfurt Center for Scientific Computing (LOEWE-CSC).

## References

- [1] H. Bando, T. Mottel, and J. Zofka, *Int. J. Mod. Phys. A* 5 (1990) 4021.
- [2] J. Schaffner, C.B. Dover, A. Gal, C. Greiner, and H. Stoecker, *Phys. Rev. Lett.* 71 (1993) 1328.
- [3] W. Greiner, *J. Mod. Phys. E* 5 (1996) 1.
- [4] O. Hashimoto, H. Tamura, *Prog. Part. Nucl. Phys.* 57 (2006) 564.
- [5] J. Schaffner-Bielich, *Nucl. Phys. A* 804 (2008) 309.
- [6] Special issue on *Progress in Strangeness Nuclear Physics*, Edt. A. Gal, O Hashimoto and J. Pochodzalla, *Nucl. Phys. A* 881 (2012) 1-338.
- [7] N. Buyukcizmeci, A.S. Botvina, J. Pochodzalla, and M. Bleicher, *Phys. Rev. C* 88 (2013) 014611.
- [8] T. Hell and W. Weise, arXiv:1402.4098 [nucl-th].
- [9] The PANDA collaboration, <http://www-panda.gsi.de> ; and arXiv:physics/0701090.
- [10] <https://indico.gsi.de/event/superfrs3> (access to pdf files via timetable and key 'walldorf')
- [11] C.Rappold, T.R. Saito, and C. Scheidenberger. Simulation Study of the Production of Exotic Hypernuclei at the Super-FRS (at GSI Scientific report 2012), GSI Report 2013-1, 176 p. (2013). <http://repository.gsi.de/record/52079> .
- [12] The STAR collaboration, *Science* 328 (2010) 58.
- [13] B. Dönigus *et al.* (ALICE collaboration), *Nucl. Phys. A* 904-905 (2013) 547c.
- [14] NICA White Paper, <http://theor.jinr.ru/twiki/cgi/view/NICA/WebHome>; <http://nica.jinr.ru/files/BM@N>.
- [15] M. Danyasz and J. Pniewski, *Philos. Mag.* 44 (1953) 348.
- [16] J.P. Bondorf, A.S. Botvina, A.S. Iljinov, I.N. Mishustin, and K. Sneppen, *Phys. Rep.* 257 (1995) 133.
- [17] H. Xi *et al.*, *Z. Phys. A* 359 (1997) 397.
- [18] R.P. Scharenberg *et al.*, *Phys. Rev. C* 64 (2001) 054602.
- [19] R. Ogul *et al.*, *Phys. Rev. C* 83 (2011) 024608.
- [20] P.B. Gossiaux *et al.*, *Nucl. Phys. A* 619 (1997) 379.
- [21] A.S. Botvina and J. Pochodzalla, *Phys. Rev. C* 76 (2007) 024909.
- [22] S.Das Gupta, *Nucl. Phys. A* 822 (2009)41; V.Topor Pop, S.Das Gupta, *Phys. Rev. C* 81 (2010) 054911.
- [23] Y.-G. Ma (for STAR/RHIC collaboration), talk at NUFRA2013 conference, Kemer, Turkey, 2013, <http://fias.uni-frankfurt.de/historical/nufra2013/>. L. Xue *et al.*, *Phys. Rev. C* 85 (2012) 064912.
- [24] P. Camerini (for ALICE/LHC collaboration), talk at NUFRA2013 conference, Kemer, Turkey, 2013, <http://fias.uni-frankfurt.de/historical/nufra2013/>.
- [25] J. Steinheimer, K. Gudima, A. Botvina, I. Mishustin, M. Bleicher, H. Stöcker, *Phys. Lett. B* 714 (2012) 85.
- [26] M. Wakai, H. Bando and M. Sano, *Phys. Rev. C* 38 (1988) 748.
- [27] Z.Rudy, W.Cassing *et al.*, *Z. Phys. A* 351 (1995) 217.
- [28] Th. Gaitanos, H. Lenske, and U. Mosel, *Phys. Lett. B* 675 (2009) 297.
- [29] A.S. Botvina, K.K. Gudima, J. Steinheimer, M. Bleicher, I.N. Mishustin, *Phys. Rev. C* 84 (2011) 064904.
- [30] J. Pochodzalla, *Prog. Part. Nucl. Phys.* 39 (1997) 443.
- [31] H. Ohm *et al.*, *Phys. Rev. C* 55 (1997) 3062.
- [32] T.A. Armstrong *et al.*, *Phys. Rev. C* 47 (1993) 1957.
- [33] T.R. Saito *et al.* (HypHI collaboration), *Nucl. Phys. A* 881 (2012) 218. C. Rappold *et al.*, *Nucl. Phys. A* 913 (2013) 170; arXiv:1305.4871.
- [34] C. Rappold *et al.*, *Phys. Rev. C* 88 (2013) 041001 (R).
- [35] A.S. Botvina, I.N. Mishustin, J. Pochodzalla, *Phys. Rev. C* 86 (2012) 011601 (R).
- [36] V.D. Toneev, K.K. Gudima, *Nucl. Phys. A* 400 (1983) 173c.
- [37] V.D. Toneev, N.S. Amelin, K.K. Gudima, S.Yu. Sivoklov, *Nucl. Phys. A* 519 (1990) 463c.
- [38] S.A. Bass *et al.*, *Prog. Part. Nucl. Phys.* 41 (1998) 225.
- [39] A.S. Botvina, K.K. Gudima, J. Pochodzalla, *Phys. Rev. C* 88 (2013) 054605.
- [40] E. L. Bratkovskaya and W. Cassing, *Nucl. Phys. A* 807 (2008) 214.
- [41] E.L. Bratkovskaya *et al.*, *Phys. Rev. C* 69 (2004) 054907.
- [42] C. Hartnack *et al.*, *Phys. Rep.* 510 (2012) 119.
- [43] W. Neubert, and A.S. Botvina, *Eur. Phys. J. A* 7 (2000) 101.
- [44] M. Bleicher *et al.*, *J. Phys. G* 25 (1999) 1859.
- [45] G. Graef, J. Steinheimer, Feng Li and M. Bleicher, to be published
- [46] W. Cassing and E. L. Bratkovskaya, *Phys. Rep.* 308 (1999) 65.
- [47] W. Cassing and S. Juchem, *Nucl. Phys. A* 665 (2000) 377; *ibid.* A 672 (2000) 417.
- [48] B. Andersson, G. Gustafson and H. Pi, *Z. Phys. C* 57 (1993) 485.
- [49] Th. Aumann, *Progr. Part. Nucl. Phys.* 59 (2007) 3.
- [50] H. Geissel *et al.*, *Nucl. Inst. Meth. Phys. Res. B* 204 (2003) 71.